Kohn Anomalies in Graphite and Nanotubes

S. Piscanec[1], M. Lazzeri[2], A. C. Ferrari[1], F. Mauri[2], J. Robertson[1]

[1]Cambridge University, Engineering Department, Cambridge, CB2 1PZ, UK
[2]Laboratoire de Mineralogie-Cristallographie de Paris, Université Pierre et Marie Curie, 75252, Paris, France

ABSTRACT

Atomic vibrations are partially screened by electrons. In a metal this screening can change rapidly for vibrations associated to certain points of the Brillouin zone, entirely determined by the shape of the Fermi surface. The consequent anomalous behaviour of the phonon dispersion is called Kohn anomaly. Graphite is a semimetal. Nanotubes can be metals or semiconductors. We demonstrate that two Kohn anomalies are present in the phonon dispersion of graphite and that their slope is proportional to the square of the electron-phonon coupling. Metallic nanotubes have much stronger anomalies than graphite, due to their reduced dimensionality. Semiconducting nanotubes have no Kohn anomalies.

INTRODUCTION

The understanding of the physical mechanisms ruling the phonon dispersions and the electron-phonon coupling in graphite is a key step to derive the vibrational properties and the Raman intensities of carbon nanotubes. A key point to understand the phonons of graphite is the semi-metallic character of its electronic structure. In general, the atomic vibrations are partially screened by electronic states. In a metal this screening can change rapidly for vibrations associated to certain q points of the Brillouin zone, entirely determined by the shape of the Fermi surface. The consequent anomalous behavior of the phonon dispersion is called Kohn anomaly [1]. Here we show that Graphite displays two remarkable Kohn anomalies at the $\mathbf{\Gamma}$-E_{2g} and $\mathbf{K}$-A'_1 modes [2]. It is also a very remarkable case, since a very simple mathematical description of the Kohn anomalies is possible. Due to their reduced dimensionality, metallic tubes display much stronger Kohn anomalies than graphite. This results in phonon softening, implying that folded graphite cannot reproduce the phonon dispersions of metallic tubes.

We perform ab-initio calculations using density functional perturbation theory within the general gradient approximation [2,3,4]. This allows the exact computation of phonon frequencies at any point of the Brillouin zone. The semi-metallic behavior of graphite is taken in account using fractional occupancy for the electronic states [5]. Calculations are done for both graphite and graphene. We use the experimental lattice parameters for graphite, a_{exp}=2.46 Å, c=6.708 Å. For graphene we use both a_{exp} and the calculated lattice parameter a_{th}= 2.479 Å. Using periodic boundary conditions, graphene is calculated separating by 7.4 Å the single graphite layers.

KOHN ANOMALIES IN GRAPHITE

Kohn anomalies are anomalous features in the phonon dispersions of metals, due to a sudden change of the electronic screening of the ionic vibrations. Their occurrence is entirely determined by the geometry of the Fermi surface. In particular,

they can happen only for phonons with a wave-vector **q**, which can connect 2 electronic states $\mathbf{k}_1$ and $\mathbf{k}_2=\mathbf{k}+\mathbf{q}$, both on the Fermi surface and such that the tangents to the Fermi surface at $\mathbf{k}_1$ and $\mathbf{k}_2$ are parallel [1].

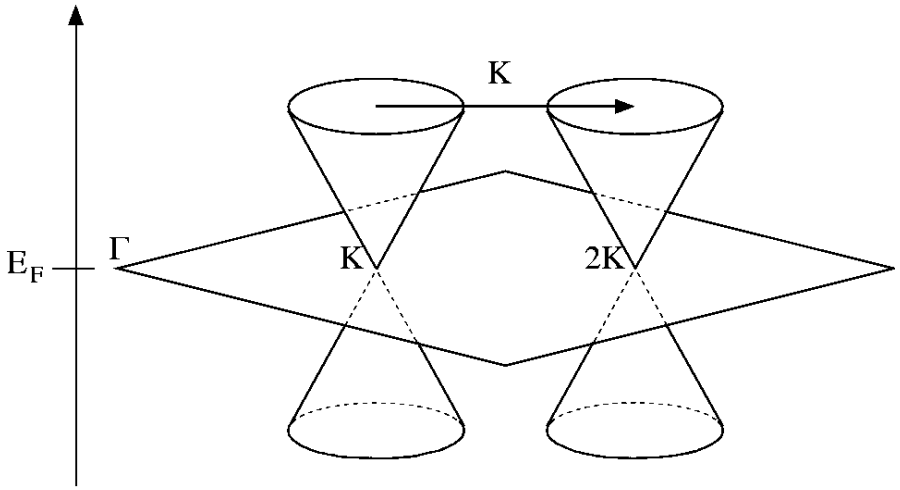

Figure 1. Schematic band structure of graphite.

The Fermi surface of graphene consists of the 2 non-equivalent **K** and **K'** points, with **K'=2K**. Kohn Anomalies can then occur for phonons connecting the **K** or **K'** points to themselves (**q=K-K=0= Γ**) or connecting **K** to **K'** (**q=K'-K=2K-K=K**). For a given **q** there are several phonon branches. In graphite, only the highest optical branches show Kohn anomalies, due to their very high electron phonon coupling [2].

The upper panel of Fig.2 shows our calculated phonon dispersions of graphite. The anomalies appear as two sharp kinks in the highest optical branches at **Γ** and **K**, corresponding to E_{2g} and A'_1 phonons. Our theoretical dispersion is compared with the experimental data of ref [6]. The experimental data in the **Γ** region are best reproduced by calculations with the experimental lattice spacing of graphite, while the data around **K** are closer to the dispersion calculated with a_{th}. However, in both cases, the difference between the experimental and calculated frequencies is less than 2%, which is the typical accuracy of density functional theory.

The presence of the two kinks in the phonon dispersion of graphene is not an artifact of the bi-dimensionality of this system. Indeed, as shown in the lower panels of Fig.2, the kinks clearly appear also in the phonon dispersion of three-dimensional graphite. In this case, the double number of atoms in the unit cell implies that a single phonon branch of graphene splits in two almost degenerate branches in graphite. This demonstrates that, for our purposes, graphene is completely equivalent to graphite.

The behavior of the anomalies around **Γ** and **K** can be described by $\hbar\varpi_q = \hbar\omega_\Gamma + \alpha_\Gamma^{LO} q + o\left(q^2\right)$ and $\hbar\varpi_{q'} = \hbar\omega_K + \alpha_K q' + o\left(q'^2\right)$. These are non-analytical functions of q and q' (q' being the phonon wavevector measured from **K**), since their first derivatives are discontinuous. Thus the Kohn anomalies cannot be reproduced using a force constants approach with a small number of force constants, as often done in literature, but would require an infinite set of force constants. However, it is possible to derive an exact analytical description of the slope of the two kinks [2]:

$$\alpha_\Gamma^{LO} = \sqrt{3}\pi^2 \left\langle g_\Gamma^2 \right\rangle_F / \beta = 397 cm^{-1} \qquad (1)$$

$$\alpha_K = \sqrt{3}\pi^2 \left\langle g_K^2 \right\rangle_F / \beta = 973 cm^{-1} \qquad (2)$$

These slopes are strictly related by:

$$\frac{\alpha_\Gamma \omega_\Gamma}{\alpha_K \omega_K} = 2 \qquad (3)$$

where $\left\langle g_\Gamma^2 \right\rangle_F$ and $\left\langle g_K^2 \right\rangle_F$ are the square of the electron phonon coupling matrix elements averaged on the Fermi surface and β=14.1 eV is the slope of the π and π^* bands near the Fermi level.

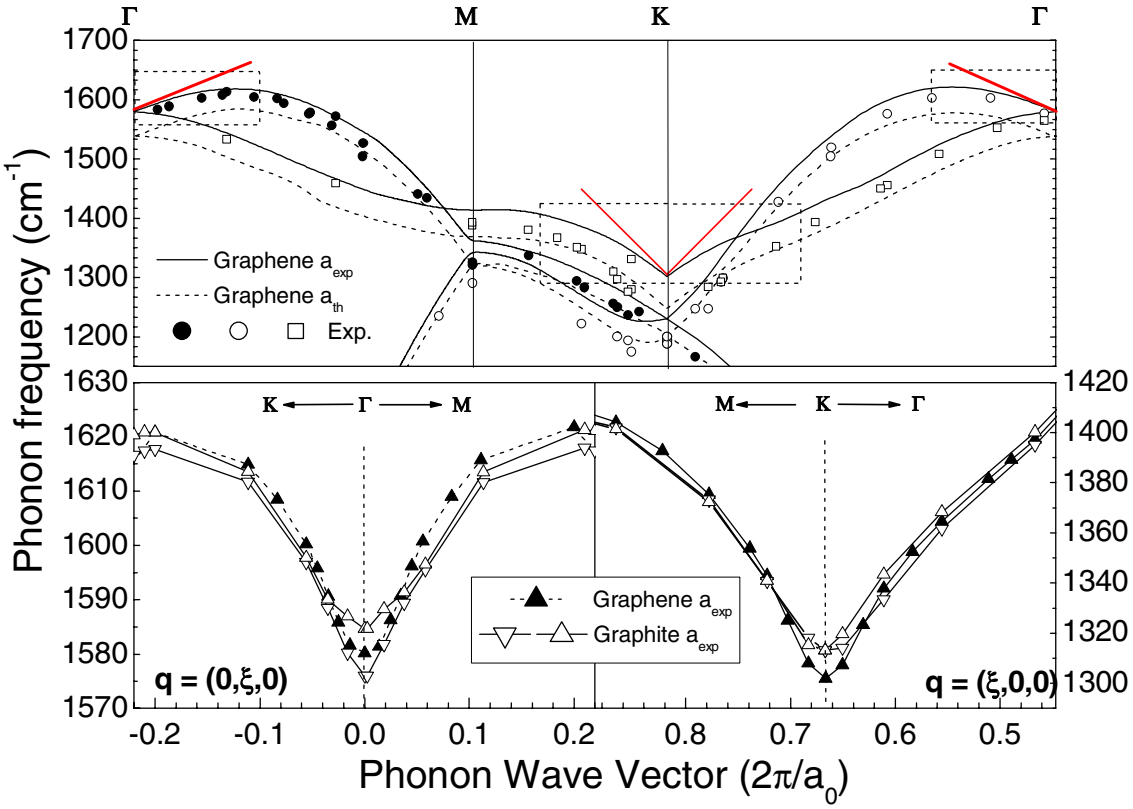

Figure 2. Upper panel: lines: phonon dispersion of graphene, calculated at the experimental (solid line) and calculated (dashed line) lattice parameter (a_{exp}, a_{th}). Points: experimental data, ref [6]. The red lines are the calculated slopes of the Kohn anomalies. The lower panels correspond to the dotted windows in the upper panel. The points are frequencies obtained by direct calculations.

In our calculations, $\left\langle g_\Gamma^2 \right\rangle_F = 0.0405 eV^2$, for the **Γ**-$E_{2g}$ mode, and zero for all the other branches at **Γ**. Similarly, $\left\langle g_K^2 \right\rangle_F$ is non negligible only for the **K**-A'$_1$ mode, for which $\left\langle g_K^2 \right\rangle_F = 0.0994 eV^2$. This confirms the attribution of the Raman D peak of disordered graphite to the highest optical branch starting from the K-A'$_1$ [7,8,9], for two main reasons. First, the A'$_1$ branch has, by far, the biggest electron-phonon coupling amongst the **K** phonons. Second, this branch is linearly dispersive. The Kohn anomaly is the physical origin of this dispersion, which is in quantitative agreement with the measured D peak dispersion [10,11]

Equations 1, 2, 3 are of fundamental importance since they allow the direct measurements of the electron phonon coupling matrix elements in graphite by fitting the slope of the measured phonon dispersions or the experimental Raman D peak dispersion. For example, Fig. 3 shows a quadratic fit to the experimental data of ref.[6]. This gives α^{LO}_{Γ}=340 cm^{-1} and $\left\langle g^2_{\Gamma} \right\rangle_F = 0.035 eV^2$, in excellent agreement

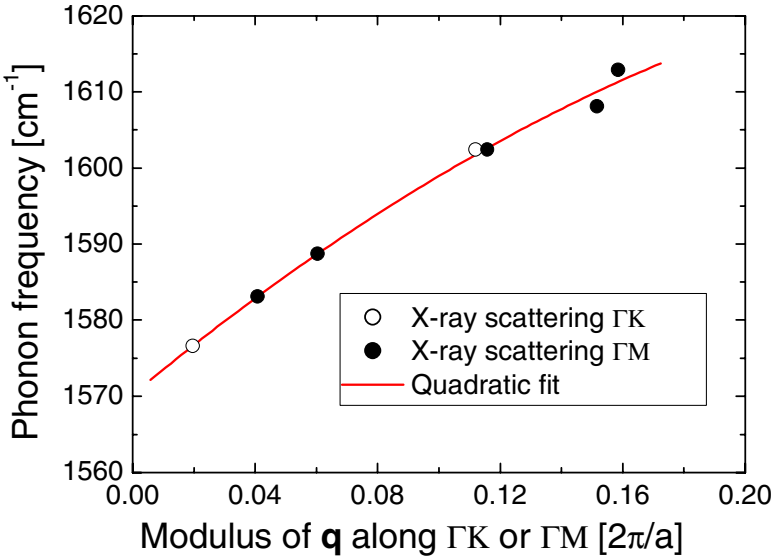

Figure 3. Fit of the experimental phonon dispersion around Γ of ref. [6]

with our calculations. We get similar results by fitting the phonon dispersions data measured by other authors by a variety of different techniques, such as electron energy loss spectroscopy and neutron scattering [2,12]. The slope at K can also be estimated from the well-known dispersion of the Raman D-peak of graphite: 50 cm^{-1}/eV [11]. The D-peak dispersion corresponds to the ratio between the slope of the phonon dispersion around **K** and β [13]. This gives $\left\langle g^2_{K} \right\rangle_F = 0.072 eV^2$. Experimentally, the D peak dispersion is measured for excitation energies higher than 1 eV, this means that the slope at **K** is ~30% higher than the measured dispersion, as shown in the upper panel of Fig. 2. Taking this into account we get $\left\langle g^2_{K} \right\rangle_F = 0.094 eV^2$, again in excellent agreement with our calculations. What is most impressive is that the experimental electron phonon coupling, albeit fitted to data measured with diverse techniques, ranging from neutron scattering to Raman spectroscopy, do satisfy equation 3. This is a very stringent relation and could not be just accidentally satisfied.

KOHN ANOMALIES IN NANOTUBES

The presence of Kohn anomalies in graphite implies that that they should be present in metallic nanotubes. The geometrical condition for the existence of the anomalies is the one-dimensional equivalent of Fig. 1. Metallic tubes have much stronger anomalies than graphite, due to their reduced dimensionality. Thus, folded graphite does not reproduce the phonon dispersions of metallic nor semiconducting nanotubes. Direct *ab-initio* calculations are necessary to properly describe nanotubes phonons, but this is practically unfeasible for nanotubes of arbitrary chirality, given their huge unit cells. We thus developed a new adaptive k-point sampling approach

[14], which allow us to efficiently and precisely calculate the phonon dispersions, the Kohn anomalies and their temperature dependence for any nanotube, independent of the unit cell size, Fig. 4

The calculated softening for armchair nanotubes depends strongly on the electronic temperature of the system. This is a completely different phenomenon from the usual temperature induced anharmonicity. Indeed the temperature dependence is

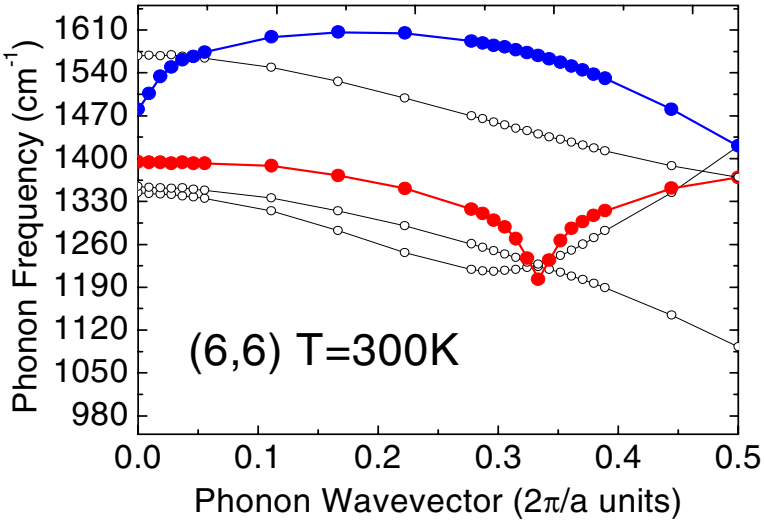

Figure 4. Highest optical branches for a (6,6) nanotube calculated at room temperature. Two strong Kohn anomalies are present for the phonons corresponding to the **Γ**-E_{2g} mode (blue dots) and the **K** -A'_1 (red dots) mode at of graphite.

the opposite of what expected as a consequence of anharmonicity. The softening also depends on the diameter of the tubes. In particular the anomalies are more intense for tubes with small diameters and for low temperature (Table I). A softening of metallic nanotubes phonons corresponding to the graphene **Γ**-E_{2g} mode was previously reported [14]. It is now clear that this is due to the presence of a Kohn anomaly. We also calculate a stronger softening for the phonons corresponding to the **K**-A'_1 mode.

	3-3		**6-6**		**11-11**	
Temp (K)	E_{2g}	A'_1	E_{2g}	A'_1	E_{2g}	A'_1
3000	1523	1299	1568	1327	1576	1330
300	1396	1111	1499	1236	1546	1277
77	1270	987	1454	1180	1522	1247
4	1031	855	1352	1056	1496	1182

Table I. calculated phonon frequencies for three (n,n) metallic carbon nanotubes as a function of electronic temperature. Phonon frequencies are in cm^{-1}

Our findings together with the ones of ref. 14 nicely account for the differences observed in the Raman spectra of metallic and semiconducting nanotubes. For metallic nanotubes, the G^- component of the G peak is red-shifted, broader and more intense than in semiconductining nanotubes [16]. We can interpret the G^- peak in metallic nanotubes as the signature of the Kohn anomaly and the presence of an intense electron phonon coupling rather than a Fano resonance, as usually done [16,17]. Indeed the experimental dependence of the G^- peak as a function of tube diameter [16] agrees with Table I [14,15] and Fig. 4.

Finally, the electron phonon coupling of nanotubes of chiral indexes (n,m) can be simply derived from the one of graphite by using [18]:

$$g_{tube} = g_{graph} \frac{\sqrt{\gcd(2n+m, 2m+n)}}{\sqrt{2\left(n^2+nm+m^2\right)}} \quad (4)$$

where gcd(2n+m, 2m+n) is the greatest common divisor between 2n+m, 2m+n.

CONCLUSIONS

We demonstrated two strong Kohn anomalies in the phonon dispersion of graphite. We gave an exact analytical description of these anomalies. The slope of the anomalies is proportional to the square of the electron phonon coupling matrix elements. This allows us to directly measure the electron phonon coupling of graphite from the experimental phonon dispersions. The electron phonon coupling of nanotubes can then simply be derived from the one of graphite, by using equation 4.

Kohn anomalies are present in metallic carbon nanotubes, but absent in semiconducting nanotubes. Interatomic force constants approaches with a finite number of force constants cannot accurately reproduce the exact shape of the phonon dispersions of graphite nor nanotubes.

ACKNOWLEDGEMENTS

We thank C. Brouder, M. Calandra and S. Reich for useful discussions. Calculations were performed at HPCF (Cambridge) and IDRIS (Orsay) using PWscf [19]. SP was supported by the EU project FAMOUS and the Marie Curie Fellowship IHP-HPMT-CT-2000-00209. ACF acknowledges funding from the Royal Society.

REFERENCES

1. W. Kohn, Phys. Rev Lett. 2, 393 (1959)
2. S. Piscanec et al, Phys. Rev. Lett. 93, 185503 (2004)
3. S. Baroni et al., Rev. Mod. Phys. 73, 515, (2001)
4. N. Troullier and J. L. Martins, Phys. Rev. B 43, 1993 (1991)
5. M. Methfessel and A.T. Paxton, Phys. Rev. B 40, 3616 (1989)
6. J. Maultzsch et al, Phys. Rev. Lett 92, 075501 (2004)
7. F. Tuinstra, J. L. Koening, J. Chem. Phys. 53, 1126 (1970).
8. C. Mapelli et al, Phys. Rev. B **60**, 12710 (1999)
9. A.C. Ferrari and J. Robertson Phys. Rev. B **61**, 14095 (2000); **64**, 075414 (2001).
10. R.P. Vidano et al., Solid State Commun. 39 341 (1981)
11. I. Poksic et al., J. Non-Cryst.Solids 227-230, 1083 (1998)
12. for a review see L.Wirtz and A. Rubio, Solid State Commun. **131**, 141 (2004).
13. C. Thomsen and S. Reich, Phys. Rev. Lett. 85, 5214 (2000)
14. S. Piscanec et al. Phys. Rev. Lett. Submitted (2004)
15. O. Dubay and G. Kresse, Phys. Rev. B 67, 035401 (2003)
16. A. Jorio et al. Phys. Rev. Lett. 90, 107403 (2003); Phys. Rev.B 65, 155412 (2002)
17. C. Jiang et al. Phys. Rev. B 66, 161404 (2002)
18. M. Lazzeri et al. cond-mat/0503278.
19. S. Baroni et al. http://www.pwscf.org